

# MRO CRISM AND MARCI OBSERVATIONS OF MARS OZONE.

**R. T. Clancy**, Space Science Institute, Boulder, CO, USA ([clancy@spacescience.org](mailto:clancy@spacescience.org)), **M. Wolff**, Space Science Institute, Boulder, CO, USA, **M. Smith**, NASA/Goddard Space Flight Center, Greenbelt, MD, USA, **B. Cantor**, Malin Space Science Systems, San Diego, CA, USA, **F. Lefèvre**, LATMOS/IPSL, Paris, France.

**Introduction:** We present distinct, yet mutually supportive, observations of Mars atmospheric ozone, as obtained from the CRISM (Compact Reconnaissance Imaging Spectrometer, [1]) and MARCI (Mars Color Imager, [2]) experiments onboard the Mars Reconnaissance Orbiter (MRO). CRISM ozone measurements are provided by 1.27  $\mu\text{m}$  airglow emission from  $\text{O}_2$  singlet delta; which indicates daytime ozone photolysis at altitudes above 5-20 km altitudes, or ozone formation over the polar winter latitudes above 40 km altitudes [3]. MARCI images ultraviolet bands within (265 nm) and longward (320 nm) of the Hartley ozone absorption band, and so provides daily global maps of ozone column density [4]. These Mars ozone data sets, which extend from late 2006 to current observations, characterize a variety of photochemical, microphysical, and dynamical processes in the Mars atmosphere. Specific processes addressed include heterogeneous chemistry on water ice clouds [5], meridional transport of atomic oxygen into the winter polar night [3, 6], high latitude water vapor variability, orbital variation of the low-to-mid latitude hygropause [7], and mesoscale dynamics within the Hellas basin [4,8]. The daily global imaging nature of the MARCI column measurements lends to an emphasis on water vapor variability as driven by seasonal supply, condensation, and transport effects. The vertical coverage of CRISM  $\text{O}_2$  singlet delta observations emphasizes specific photochemical and microphysical processes within the middle atmospheric region of Mars.

**CRISM  $\text{O}_2$  Singlet Delta Observations:** Mars 1.27  $\mu\text{m}$  emission is associated with the electronically excited singlet delta state of  $\text{O}_2$ , which is created when ozone is photolyzed or when it is created by three body recombination of atomic oxygen. The former process predominates for sun-lighted altitudes below 40 km and can provide a fairly direct measure of ozone abundance. The latter mechanism predominates at altitudes above 40 km, where atomic oxygen is more abundant, and is particularly prominent in the polar winter night. CRISM observations of  $\text{O}_2$  singlet delta airglow consist of vertically integrated emission rates present in the standard surface spectral imaging observations, and vertical profile emission rates obtained from special limb imaging observations obtained with some regularity since the beginning of 2010.

*Polar  $\text{O}_2$  Singlet Delta Nightglow.* CRISM limb observations began in July of 2009 ( $L_s=301^\circ$ ) and have been obtained roughly every two months ( $30^\circ$

of  $L_s$ ) since February of 2010. One striking aspect of observed 1.27  $\mu\text{m}$  limb emission is the presence of a high altitude (>40 km) source in the un-illuminated (fall/winter/spring) polar ( $65$ - $90^\circ$  N/S) atmosphere. This source relates to the transport of high altitude atomic oxygen, produced at sun-lighted latitudes, into the polar fall/winter/spring atmosphere where it descends to ~50 km and recombines to form electronically excited (singlet delta) molecular oxygen. Hence, the temporal (daily, seasonal) and spatial (altitude, latitude, longitude) variation of the resulting 1.27  $\mu\text{m}$  airglow reflects upon poorly constrained meridional transport into the polar

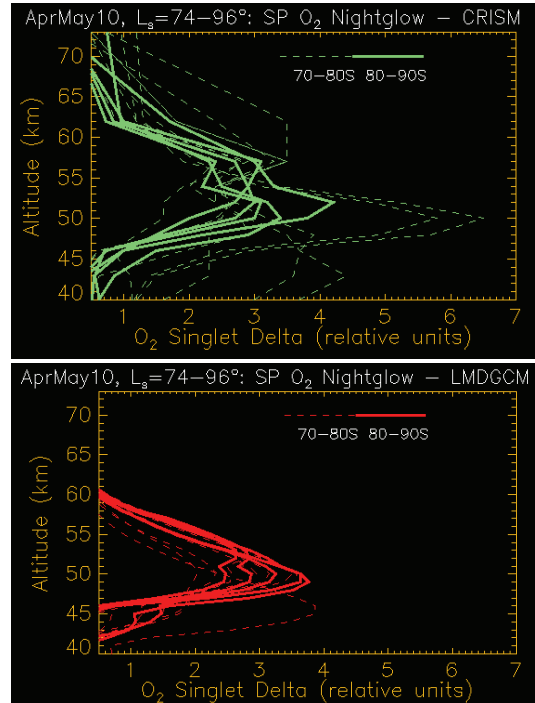


Figure 1: A comparison of CRISM observed (top panel) and LMDGCM simulated (bottom panel) polar night  $\text{O}_2$  singlet delta VER profiles for the  $L_s$  period  $74$ - $96^\circ$  (corresponding to CRISM multiple orbit of limb observations during April-May, 2010). Dashed lines indicate 70-80S latitudes, solid lines indicate 80-90S latitudes. Data-model agreement is good at 80-90S latitudes, less good at 70-80S latitudes.

fall/winter/spring atmosphere.

Figure 1 presents vertical profiles of retrieved  $\text{O}_2$  singlet delta volume emission rates (VER) for the southern polar winter, as observed in CRISM limb profiles on April 7, 28 ( $L_s=74^\circ, 83^\circ$ ) and May 26 ( $L_s=96^\circ$ ) of 2010. Solid lines indicate latitudes of 80-

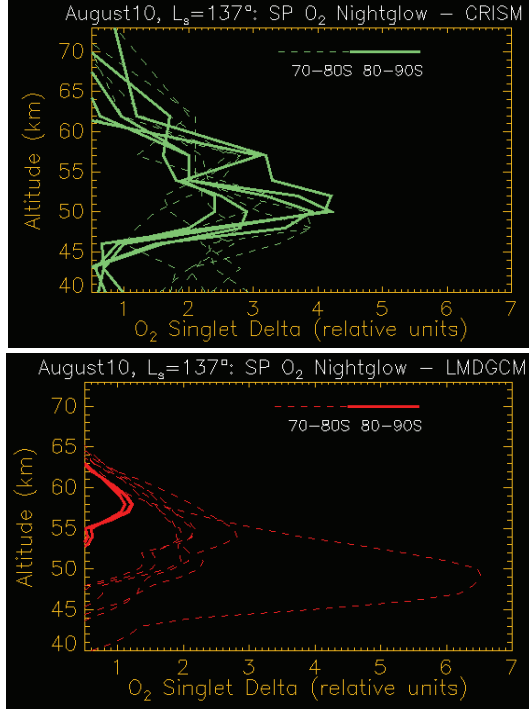


Figure 2: A comparison of CRISM observed (top panel) and LMDGCM simulated (bottom panel) polar night  $O_2$  singlet delta VER profiles for the  $L_s$  period  $137^\circ$  (corresponding to CRISM multiple orbit of limb observations on August 22-23, 2010). Dashed lines indicate 70–80S latitudes, solid line indicate 80–90S latitudes. Data-

90S, dashed lines indicate latitudes of 70–80S. The lower latitude range presents much stronger variability in  $O_2$  singlet delta intensity as well as its vertical dependence, in this southern winter solstice season. The vertical resolution of these retrievals is 2 km over the 46–56 km altitude region, within which the  $1.27 \mu\text{m}$  emission generally peaks. Figure 1b presents model simulations for the same locations and times ( $L_s$  and LT) of the CRISM observations, employing the LMDGCM photochemical model [5]. In general, the comparison is quite good, other than that the observed  $O_2$  emission profiles exhibit larger variability at 70–80S latitudes, and somewhat broader altitude distributions.

However, Figure 2 indicates reduced model-data agreement for the late southern winter period ( $L_s=137^\circ$ ), particularly at 80–90S. The model predicts a significant decrease in  $O_2$  singlet delta emission poleward of 80S whereas the observations exhibit modest poleward increases in  $O_2$  singlet delta emission, similar to the  $L_s=74$ – $96^\circ$  period of figure 1. Over the full  $L_s=50$ – $137^\circ$  period of observation in 2010, the observations present larger variability, longitudinal gradients, and poleward increases relative to the model predictions. These comparisons, however, are in the preliminary stages.

*$O_2$  Singlet Delta Dayglow.* For each of the CRISM limb observing periods, we obtained latitu-

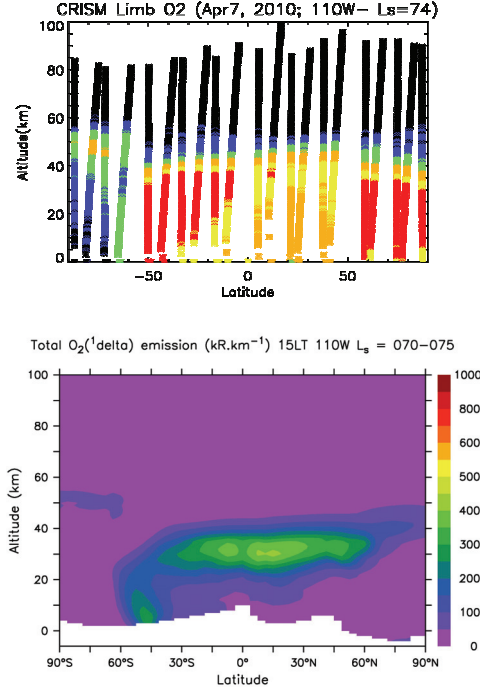
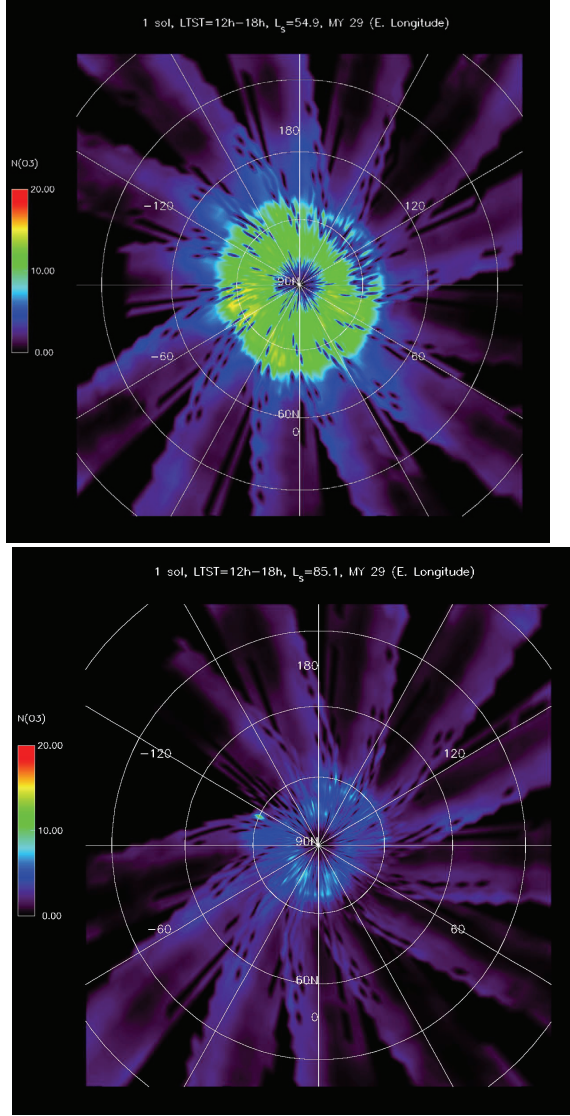


Figure 3: Latitude-altitude cross section of CRISM observed limb radiances (top panel) and LMDGCM simulated VER for  $O_2$  singlet delta dayglow (and polar nightglow at south polar region), on April 7, 2010 ( $L_s=74^\circ$ ) along an orbit centered on the Tharsis ridge (110W). Intense  $O_2$  singlet delta emission over the northern spring cap appears only in the observations., indicating higher ozone abundances over the cap than simulated by the model

dinal cross sections centered on 110W and 300W equatorial longitudes (although there is variable coverage loss among these data). These sun-lighted  $O_2$  singlet delta observations pertain to  $O_3$  photolysis rates, and so reflect on  $O_3$  abundances directly and water vapor abundances indirectly. These data also provide spectral coverage of aerosol (dust and ice) scattering and gas ( $H_2O$ ,  $CO$ ,  $CO_2$ ) absorptions over the 0.4–3.8  $\mu\text{m}$  wavelength range. This can support key correlative studies, such as for heterogeneous chemistry, but requires more extensive radiative transfer modeling (multiple scattering limb RT) than associated with the polar night  $O_2$  singlet delta observations.

Nevertheless, inspection of the raw limb radiance profiles in terms of latitude-altitude cross-sections of  $O_2$  singlet delta emission indicates departures from model predictions over summer northern polar latitudes. Figure 3 compares the observed limb  $O_2$  singlet delta emission (upper-relative units) to model  $O_2$  singlet delta emission (lower-VER) for the April 7, 2010 ( $L_s=74^\circ$ ) period, over a longitude of 110W (Tharsis region). The most significant disagreement appears over high northern latitudes, where intense  $O_2$  singlet delta emission in the CRISM observations implies significantly larger  $O_3$  (hence, lower water vapor) abundances below 35 km relative to the mod-



el prediction for this early summer season in the north. This observed O<sub>2</sub> emission behavior in the northern is present earlier (February 10, L<sub>s</sub>=50°), but

Figure 4: MARCI image maps of column O<sub>3</sub> column density ( $\mu\text{m}\text{-atm}$ ) as constructed from 1 sol of MRO orbits on April 6 (upper panel-L<sub>s</sub>=55°) and June 14 (lower panel-L<sub>s</sub>=85°) in 2008. O<sub>3</sub> column densities over the northern late spring/early summer ice cap decrease substantially over this period, and provide general correspondence with CRISM limb profiles of O<sub>2</sub> singlet delta emission at 0-35 km altitude over the northern seasonal ice cap during the same L<sub>s</sub> range (figure 3).

decreases substantially from L<sub>s</sub>=83° (April 28) to L<sub>s</sub>=95° (May 26) in the CRISM limb observations.

**MARCI O<sub>3</sub> Daily Mapping Observations:** The continuous decline of these high O<sub>3</sub> abundances over northern high latitudes between L<sub>s</sub>=45° and 90° is well characterized in MARCI daily global O<sub>3</sub> col-

umn maps obtained in 2008 (and 2010, but not currently processed). Radiative transfer processing of the MARCI UV channel radiances is ongoing, such that preliminary column O<sub>3</sub> retrievals are under assessment with regard to providing more accurate algorithm treatments of input O<sub>3</sub> and cloud profile distributions based upon the LMDGCM simulations. Nevertheless, the current retrieval results provide a number of robust measurements, including the evolution of high latitude O<sub>3</sub> columns from spring to fall, and daily variations in Hellas basin O<sub>3</sub> column distributions [4,8]. In figure 4, we present color contour polar plots of O<sub>3</sub> column densities retrieved from MARCI UV images on April 6 (upper panel-L<sub>s</sub>=55°) and June 14 (lower panel-L<sub>s</sub>=85°) in 2008. The substantial decay in column O<sub>3</sub> (in  $\mu\text{m}\text{-atm}$ ) within the daily sequence of these MARCI O<sub>3</sub> column maps provides a nice correspondence with CRISM limb O<sub>2</sub> singlet delta profiling over the L<sub>s</sub>=40-165 range in 2010, as well as constraints on LMDGCM simulations of O<sub>3</sub> and water vapor over the spring-to-fall evolution of the northern (and corresponding southern) seasonal and residual polar cap regions of Mars.

**References:** [1] Murchie, S., et al., JGR, 12, E05S03, doi:10.1029/2006JE002682, 2007. [2] Malin, M., et al., Icarus, 194, 501-512, 2008. [3] Clancy, R. et al., Bull. Amer. Astron. Soc., 42, p. 1041, 2010. [4] Wolff, M., et al., Bull. Amer. Astron. Soc, 42, p. 1028, 2010. [5] Lefèvre et al., Nature, 454, 305-309, 2008. [6] Bertaux, J.-L., et al., Bull. Amer. Astron. Soc., 42, p. 1040., 2010. [7] Clancy and Nair, JGR, 101, 12785-12790, 1996. [8] Clancy, R., et al, Fall AGU, San Francisco, December 2010.